Canola seed or not? Autoencoder-based Anomaly Detection in Agricultural Seed Production

Maksim Kukushkin[1], Matthias Enders[2], Reinhard Kaschuba[3], Martin Bogdan[4] and Thomas Schmid[5]

Abstract: Analysing harvested seeds is a time-consuming task in the seed-producing industry. Automating this process has the potential to enhance and expedite agricultural seed production. In our study, we focus on differentiating Canola seeds from visually similar non-Canola seeds using computer vision techniques. Our approach utilises both RGB and hyperspectral images, captured by a specialised camera, to train separate autoencoder neural networks. By leveraging the high spatial resolution of RGB data and the high spectral resolution of hyperspectral data, we develop distinct models for Canola seed analysis, ensuring a comprehensive and robust assessment. The autoencoder networks are trained on a dataset of Canola seeds, allowing for the extraction of latent representations from both RGB and hyperspectral data. This enables efficient compression of input data and effective discrimination between Canola and non-Canola seeds. Our proposed approach demonstrates promising results in detecting non-Canola seeds in unseen test data.

Keywords: anomaly detection, seed production, hyperspectral imaging, autoencoder

1 Introduction

In agricultural seed production, classifying and sorting harvested seeds is ultimately required for quality assurance. At the same time, however, this task is also particularly challenging and requires years of expertise and training for human analysts. Using rapeseed as a sample case, we are developing an AI-supported platform for the classification and sorting of plant seeds and seed purity. To this end, we aim to integrate advanced machine learning techniques with robotic sensors and actors into a unified, continuously learning sorting platform. It will establish sorting as a collaborative process between users and the learning algorithm in order to significantly increase its efficiency in comparison to manual testing.

From a computational point of view, the central task of this approach is the computer vision task of anomaly detection. This task plays a vital role in both human and machine intelligence

[1] Leipzig University, Institute of Computer Science, Augustusplatz 10, 04109 Leipzig, Germany kukushkin@informatik.uni-leipzig.de
[2] NPZ Innovation GmbH, Hohenlieth-Hof, 24363 Holtsee, Germany m.enders@npz-innovation.de
[3] Hochschule Bielefeld - University of Applied Sciences and Arts, Interaktion 1, 33619 Bielefeld, Germany reinhard.kaschuba@hsbi.de
[4] Leipzig University, Institute of Computer Science, Augustusplatz 10, 04109 Leipzig, Germany bogdan@informatik.uni-leipzig.de
[5] Martin-Luther-Universität Halle-Wittenberg / Lancaster University in Leipzig / Leipzig University, Germany thomas.schmid@medizin.uni-halle.de

by identifying unusual or unexpected patterns in data. It holds significant importance across diverse domains such as science, engineering, finance, healthcare, cybersecurity, and more. Anomaly detection is crucial for identifying outliers or deviations from the expected behaviour, enabling timely intervention and decision-making in various applications and disciplines.

Here, we apply anomaly detection techniques in the context of agricultural production of Canola seed (scientifically known as *Brassica napus* L./Rape seed). As Canola seeds play a crucial role in ensuring global food security [AA; He20], the presence of weeds in oilseed rape fields during the harvest presents a significant challenge. It complicates the seed sorting process and compromises the accuracy of regulatory purity testing during seed production. To tackle this issue, we propose an anomaly detection system specifically designed for differentiating Canola from non-Canola seeds using hyperspectral and RGB images. In this paper, we assess this approach for Canola seeds and samples of three commonly encountered weed species by conducting comprehensive anomaly detection analyses.

2 Related Work

Anomaly detection for images is an important area of research with broad applications in various fields [Pi14]. Recently, there has been increasing attention to the development of unsupervised anomaly detection methods that do not rely on labelled data. The three arguably most widely used approaches employed for anomaly detection are autoencoders, generative adversarial networks and transfer learning with convolutional neural networks.

In the context of anomaly detection, an autoencoder (AE) may be trained using a collection of normal images and subsequently applied to analyse new, unseen images. If the AE struggles to reconstruct an input image accurately, it is identified and classified as an anomaly. A vanilla AE may, however, struggle to reconstruct complex image features, such as textures and patterns, which can lead to false positives or false negatives. To address this limitation, researchers have proposed various modifications to the AE architecture, such as using denoising AEs [Lu17] or adding regularisers to the loss function [AC15; Ma15; Ri11; Vi08] to improve their reconstruction accuracy and anomaly detection performance.

Generative adversarial networks (GANs) models [AAB19; Sc17; Sc19] may be used to characterise the normal distribution of the data and subsequently identify anomalies as samples that significantly deviate from this distribution. However, GAN approaches present certain challenges in their training process, such as failure to converge and mode collapse [Me16]. Additionally, distinguishing abnormal samples from the generative distribution poses difficulties, affecting the performance [AAB19]. Another popular approach is transfer learning, where pre-trained CNNs are fine-tuned on anomaly detection tasks [An16; De21; Ro22]. This approach has been shown to be effective in detecting anomalies in new domains with limited labeled data availability. However, due to the disjointed feature extraction and anomaly scoring could lead to suboptimal results [Pa21].

3 Methodology

Due to its simplicity, speed, and established performance, we selected an autoencoder (AE) architecture as the foundation for the anomaly detection system. The availability of sufficient training data, too, was supporting this decision. The AE operates in two stages: Initially, it takes an input image, represented as r_i, and compresses it into a lower-dimensional representation. In the subsequent stage, the AE aims to reconstruct the input image with the highest accuracy. The loss function, which measures the difference between the reconstructed image r_i' and the input image r_i, is defined as follows:

$$MSE = \frac{1}{n}\sum_{i=1}^{n}(r_i - r_i')^2 \tag{1}$$

where r_i and r_i' denote the input and reconstructed images, respectively.

Considering the presence of two types of data, namely hyperspectral data with high spectral resolution but low spatial resolution, and RGB data with low spectral resolution but high spatial resolution, we propose to employ two separate autoencoder-based models tailored to each data type, namely RGB-AE and HS-AE with latent dimension of 4096 (see. Fig 1).

It is important to note that our HS-AE differs from RGB-AE in its architecture. In addition to Conv2D and fully connected layers (similar to RGB-AE), HS-AE also incorporates Conv3D layers to extract spatio-spectral information (refer to Fig. 1b). To enable the use of RGB images as input, we standardised their size by resizing or padding them to a consistent dimension of 192x192 pixels. Furthermore, for the sake of computational efficiency in HS-AE, a hyperspectral region of interest was extracted from the centre of the hyperspectral images, specifically with a volume of 16x16x300.

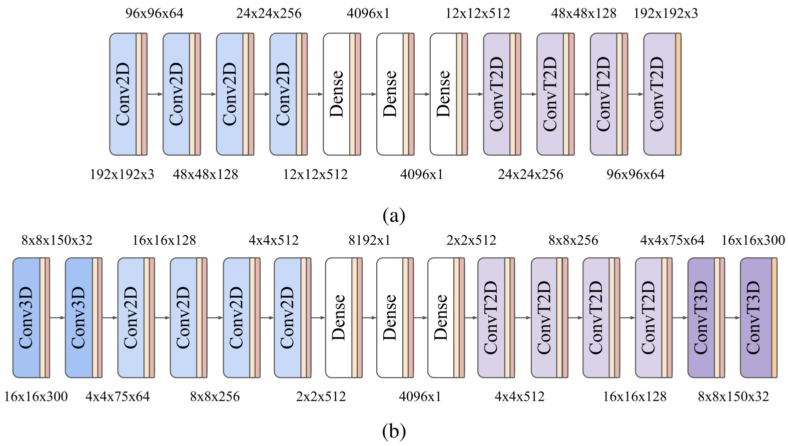

Fig. 1: Architectures of RGB-AE (a) and HS-AE (b). Please note, for RGB-AE and HS-AE use BatchNorm (yellow) and LeakyReLU (red)

4 Experiments

Data. The training dataset utilised in our study comprises a total of 3,156 RGB images along with their corresponding 3,156 hyperspectral images of Canola. For the purpose of testing, we have a separate set containing 370 images, out of which 280 belong to the normal class (*Brassica napus* L.). The remaining 90 images in the test set are equally distributed among three distinct weed species: *Anchusa arvensis* L., *Sinapis alba* L., and *Sinapis arvensis* L. (see Fig. 2). Hence, the primary objective of our anomaly detection approach is to accurately identify these 90 images from the anomalous class. The corresponding hyperspectral images are composed of 300 wavelengths within the visible and near-infrared (VNIR) range of the electromagnetic spectrum (380 - 1000 nm) (see Fig. 3).

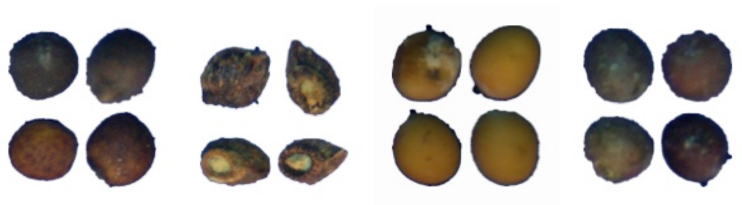

(a) (b) (c) (d)

Fig. 2: Examples of images from the test dataset. (a) Represents the normal class, showing images of *B. napus*, (b-d) Depict anomalous classes, displaying images of *Anchusa arvensis* L., *Sinapis alba* L., and *Sinapis arvensis* L. respectively.

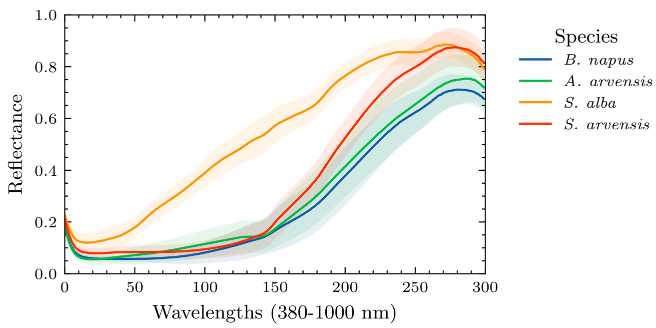

Fig. 3: Mean spectra with standard deviation for each seed species in test dataset

Training setting. Both the RGB-AE and HS-AE models were trained using the same configuration. This configuration involved training with the Adam optimizer, using a learning rate of 0.001 for 100 epochs with a learning rate schedule. A batch size of 128 was employed, and various data augmentation techniques, such as vertical and horizontal flips, as well as rotations, were applied to augment the training dataset and expand its size. To compare the performance of the two models, we employed several evaluation metrics, including (i) the Area Under the Receiver Operating Characteristic Curve (AUC), (ii) Accuracy, (iii) Sensitivity, (iv) Specificity and (v) weighted F1-Score. In our study, we determined the threshold by using the ROC curve, as the selection of this threshold can lead to significant variations in metrics (ii) to (iv).

Results. As illustrated in Fig. 4a, the HS-AE exhibits an AUC score of 0.96, surpassing the score of 0.90 achieved by the RGB-AE. The optimal thresholds determined by analysing the ROC curve are 7.7191×10^{-3} for the RGB-AE and 8.5624×10^{-4} for the HS-AE. Upon closer inspection of the Table 1, it can be observed that the specificity of the RGB-AE is only slightly higher than that of the HS-AE, reaching 0.857. However, the HS-AE demonstrates a significantly higher sensitivity of 0.941. Furthermore, the F1-Score is also superior for the HS-AE, measuring 0.881 as opposed to 0.845 for the RGB-AE. Similarly, the accuracy, as illustrated in Figure 4b, shows that the HS-AE achieves 0.875, which is 0.35 higher than the accuracy achieved by the RGB-AE.

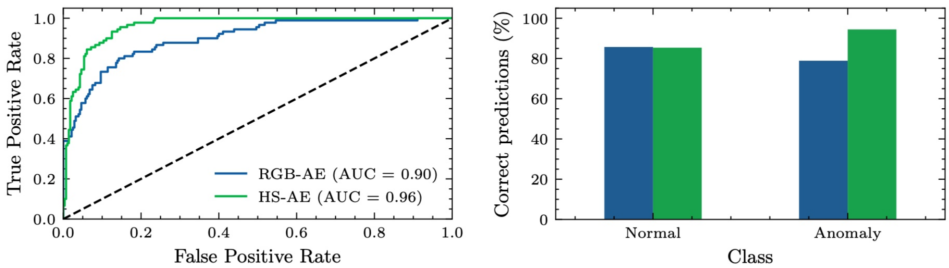

(a) (b)

Fig. 4: Comparison of the performance between RGB-AE (blue) and HS-AE (green): (a) ROC curve and Area under the ROC curve, and (b) Number of correctly detected images.

	Accuracy	Sensitivity	Specificity	F1-score	AUC
RGB-AE	0.840	0.788	**0.857**	0.845	0.897
HS-AE	**0.875**	**0.944**	0.853	**0.881**	**0.961**

Tab. 1: Evaluation metrics of RGB-AE and HS-AE

5 Discussion

Results from training and testing demonstrate the reliability of our approach for differentiating Canola from non-Canola seeds. In order to gain deeper insights, we conducted a thorough analysis to identify the specific types of anomalies where the HS-AE and RGB-AE made the highest number of incorrect predictions. Our findings, depicted in Fig. 5, reveal that both models performed remarkably well in detecting anomalies associated with the species *S. alba* with the HS-AE model correctly detecting all images of this species.

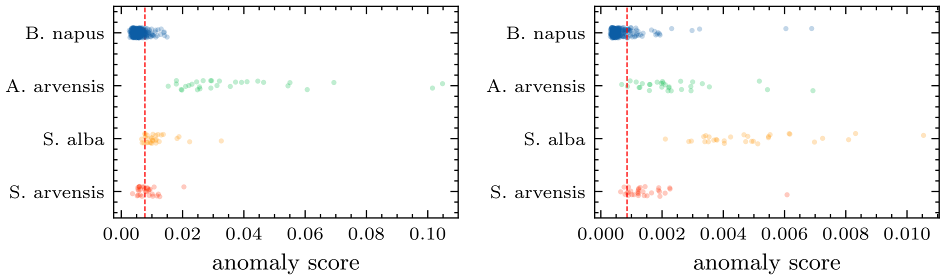

(a) (b)

Fig. 5: Reconstruction error distributions (anomaly scores) for test datasets generated by RGB-AE (a) and HS-AE (b), using MSE. The dashed red line indicates the threshold.

On the other hand, the RGB-AE model successfully detected all images associated with the *A. arvensis*, but encountered difficulties in detecting anomalies related to *S. arvensis*. This difficulty can be attributed to the visual similarities between *B. napus* and *S. arvensis*. However, by utilising hyperspectral data, it becomes possible to effectively distinguish between these two species. The aforementioned findings highlight the superiority of the HS-AE, as it outperformed the RGB-AE across almost all evaluation metrics. This indicates that the spectral information of plant seeds holds greater importance than the spatial information for the most cases.

6 Conclusion and Outlook

In conclusion, we strongly believe that AI has a crucial role to play in promoting sustainability in agriculture. By automating routine processes and reducing errors, AI simplifies the lives of agricultural workers. Our system specifically focuses on seed production and aids in ensuring seed purity, a task traditionally performed by humans. By incorporating AI technology, we can enhance the efficiency and accuracy of this process, ultimately contributing to a more sustainable agricultural industry.

In this study, we successfully demonstrated the effectiveness of autoencoders (AE) in differentiating Canola from non-Canola seeds using RGB and hyperspectral images. The results highlight the potential of our approach to optimize and accelerate agricultural seed production.

Moving forward, our future work aims to advance anomaly detection techniques in agriculture. We plan to integrate the strengths of RGB imagery and hyperspectral data, leveraging both approaches to achieve more accurate anomaly detection. Furthermore, we will identify key wavelengths that provide valuable information for distinguishing different types of plant seeds. This will simplify the anomaly detection process, increase efficiency, and potentially reduce costs.

Acknowledgements

This study was carried out as part of the project KIRa funded by the German Ministry of Food and Agriculture (BMEL, FKZ 28DK116A20).

We express our gratitude to NPZ Innovation GmbH for generously providing the dataset, without which this research would not have been possible.

References

[AA] Agriculture Department, N.; Agriculture, U.: Agricultural Statistics, 2002 (Paperback). U.S. Government Printing Office, ISBN: 9780160869273.

[AAB19] Akcay, S.; Atapour-Abarghouei, A.; Breckon, T. P.: GANomaly: Semi-supervised Anomaly Detection via Adversarial Training. In: Computer Vision – ACCV 2018. Springer International Publishing, pp. 622–637, 2019, URL: https://doi.org/10.1007/978-3-030-20893-6_39.

[AC15] An, J.; Cho, S.: Variational autoencoder based anomaly detection using reconstruction probability. Special lecture on IE 2/1, pp. 1–18, 2015, URL: http://dm.snu.ac.kr/static/docs/TR/SNUDM-TR-2015-03.pdf.

[An16] Andrews, J.; Tanay, T.; Morton, E. J.; Griffin, L. D.: Transfer representation-learning for anomaly detection. In. JMLR, 2016.

[De21] Defard, T.; Setkov, A.; Loesch, A.; Audigier, R.: PaDiM: A Patch Distribution Modeling Framework for Anomaly Detection and Localization. In: Pattern Recognition. ICPR International Workshops and Challenges. Springer International Publishing, pp. 475–489, 2021, URL: https://doi.org/10.1007/978-3-030-68799-1_35.

[He20] Heuzé, V.; Tran, G.; Sauvant, D.; Lessire, M.; Lebas, F.: Rapeseeds, https://www.feedipedia.org/node/15617, [Online; accessed 2023-05-23], Jan. 2020.

[Lu17] Lu, W.; Cheng, Y.; Xiao, C.; Chang, S.; Huang, S.; Liang, B.; Huang, T.: Unsupervised Sequential Outlier Detection With Deep Architectures. IEEE Transactions on Image Processing 26/9, pp. 4321–4330, Sept. 2017, URL: https://doi.org/10.1109/tip.2017.2713048.

[Ma15] Makhzani, A.; Shlens, J.; Jaitly, N.; Goodfellow, I.; Frey, B.: Adversarial Autoencoders, 2015, URL: https://arxiv.org/abs/1511.05644.

[Me16] Metz, L.; Poole, B.; Pfau, D.; Sohl-Dickstein, J.: Unrolled Generative Adversarial Networks, 2016, URL: https://arxiv.org/abs/1611.02163.

[Pa21] Pang, G.; Shen, C.; Cao, L.; Hengel, A. V. D.: Deep Learning for Anomaly Detection. ACM Computing Surveys 54/2, pp. 1–38, Mar. 2021, URL: https://doi.org/10.1145/3439950.

[Pi14] Pimentel, M. A.; Clifton, D. A.; Clifton, L.; Tarassenko, L.: A review of novelty detection. Signal Processing 99/, pp. 215–249, June 2014, URL: https://doi.org/10.1016/j.sigpro.2013.12.026.

[Ri11] Rifai, S.; Vincent, P.; Muller, X.; Glorot, X.; Bengio, Y.: Contractive Auto-Encoders: Explicit Invariance during Feature Extraction. In. ICML'11, Omnipress, Bellevue, Washington, USA, pp. 833–840, 2011, ISBN: 9781450306195.

[Ro22] Roth, K.; Pemula, L.; Zepeda, J.; Schölkopf, B.; Brox, T.; Gehler, P.: Towards total recall in industrial anomaly detection. In: Proceedings of the IEEE/CVF Conference on Computer Vision and Pattern Recognition. Pp. 14318–14328, 2022, URL: https://openaccess.thecvf.com/content/CVPR2022/papers/Roth_Towards_Total_Recall_in_Industrial_Anomaly_Detection_CVPR_2022_paper.pdf.

[Sc17] Schlegl, T.; Seeböck, P.; Waldstein, S. M.; Schmidt-Erfurth, U.; Langs, G.: Unsupervised Anomaly Detection with Generative Adversarial Networks to Guide Marker Discovery. In: Lecture Notes in Computer Science. Springer International Publishing, pp. 146–157, 2017, URL: https://doi.org/10.1007/978-3-319-59050-9_12.

[Sc19] Schlegl, T.; Seeböck, P.; Waldstein, S. M.; Langs, G.; Schmidt-Erfurth, U.: f-AnoGAN: Fast unsupervised anomaly detection with generative adversarial networks. Medical Image Analysis 54/, pp. 30–44, May 2019, URL: https://doi.org/10.1016/j.media.2019.01.010.

[Vi08] Vincent, P.; Larochelle, H.; Bengio, Y.; Manzagol, P.-A.: Extracting and composing robust features with denoising autoencoders. In: Proceedings of the 25th international conference on Machine learning - ICML '08. ACM Press, 2008, URL: https://doi.org/10.1145/1390156.1390294.